CASL-U-2012-0012-000

Power uprates
and plant life extension

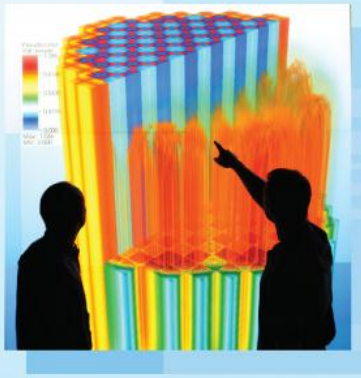

Engineering design
and analysis

Science-enabling
high performance
computing

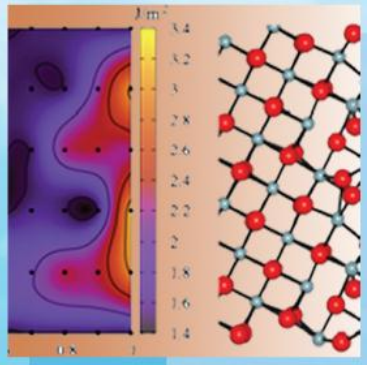

Fundamental science

Plant operational data

Consortium for Advanced Simulation of LWRs

L3:THM.ITM.P4.02

Igor Bolotnov
NCSU

Completed: 1/31/12

U.S. DEPARTMENT OF ENERGY | Nuclear Energy

ITM Simulations of Subcooled Flow Nucleate Boiling Experiment at TAMU

L3:THM.ITM.P4.02 milestone report

Igor A. Bolotnov, North Carolina State University

Carlos E. Estrada-Perez, Texas A&M University

Yassin A. Hassan, Texas A&M University

31 January 2012 (Ver. 1.0)

CASL-U-2012-0012-000

Abstract: A set of challenge simulations are formulated by CASL-THM members based on anticipated experimental data generated by CASL-supported facilities at MIT, TAMU and CCNY. This report overviews the Texas A&M experimental facility and defines a set of interface tracking methods (ITM) challenge simulations to be performed at experimental conditions in order to validate the performance of ITM codes and produce detailed numerical database for boiling two-phase flows.

Contents

LIST OF FIGURES 4

LIST OF TABLES 4

1. RELEVANCE TO CASL AND OBJECTIVES 5

2. EXPERIMENT AND SIMULATION DESCRIPTION 5

2.1 Detailed experimental description 5

Geometry 5

Operational Conditions 6

2.2 Assumptions/Scaling/Approximations 8

2.2.1 Fluid selection and scaling 8

3. SIMULATION DEFINITION 9

3.1 Operating conditions 9

3.2 Domain 9

3.3 Boundary conditions 10

3.3.1. Conjugate Heat Transfer 11

3.3.2. Single-phase turbulent inflow boundary condition 12

3.4 Initial conditions 12

3.5 Grid Size 12

3.5.2. Bubble resolution requirements-based mesh 13

3.5.3. Mesh Adaptivity 13

Advanced meshes for nucleating bubbles 13

3.5.4. Proposed cases which fully resolve both turbulence and bubbles 14

No-phase-change case: 15

Preliminary validation case: 15

Large scale simulation: 16

Detailed bubble resolution simulation: 16

4. REQUESTED CALCULATIONS AND METRICS 17

5. UPSCALE OF RESULTS TO MULTIPHASE CFD LEVEL 18

BIBLIOGRAPHY 19

List of Figures

Fig. 1. Schematics of Test Section. 6
Fig. 2. High speed visualization of nucleation sites to estimate average departure bubble diameters. 8
Fig. 3. Important operation conditions and corresponding values for HFE-301 refrigerant and water. 9
Fig. 4. Two-phase computational domain geometry and axis orientation 10
Fig. 5. Cross-section view of the ITO heater (red line) and insulating glass (pink rectangle), air gap (white) and Barium Fluoride window (green). Bubble pattern shown only for the purpose of designating the two-phase flow region. 11
Fig. 6. High speed Boroscope visualization of boiling bubbles on the non-heated section 15
Fig. 7. Zoom images of nucleation sites located at (a) six hydraulic diameters, (b) 9 hydraulic diameters from the start of heating. 16

List of Tables

Table 1. Relevant experimental dimensions. 6
Table 2. Experimental conditions at onset of nucleate boiling. 6
Table 3. Experimental parameters compared with PWR conditions. 7
Table 4. Summary of the models and correlation of bubble diameters in a vertical forced convective boiling 7
Table 5. Measured bubble departure diameters 8
Table 6: Important operation conditions and corresponding values for HFE-301 refrigerant and water ... 9
Table 7. Computational domain boundaries 10
Table 8. Estimated grid resolutions based on the different Reynolds numbers. 13
Table 9. Bubble-sized based resolution estimates: 13
Table 10. Adaptive meshing requirements for individual nucleation sites. 14
Table 11. Measured bubble diameters at 40 D_h downstream the heated section 15
Table 12. Summary of the challenge simulation cases. 17

1. Relevance to CASL and Objectives

We will define a set of simulations of nucleate boiling in turbulent flow in a vertical channel that will result in detailed information about the rate at which vapor bubbles form and grow, how they depart and move along and away from the wall, and how and where they recondense as they move into the colder liquid. The simulation will be designed to resolve all relevant continuum length and time-scales -- with fully validated subgrid models only used for the initial nucleation and the microlayer beneath vapor bubbles -- using the maximum number of grid points feasible and a sufficiently large number of time steps to ensure that meaningful statistical quantities can be obtained. The simulation will result in a detailed picture of heat transfer at the wall as well as the effect of boiling on the flow. The objective of the simulation is to generate a numerical database from which closure relations for upscale codes (multiphase CFD with turbulence modeling) can be extracted at the conditions of interest to two CASL challenge problems (i.e. CRUD and DNB).

2. Experiment and simulation description

A summary of the unique features of the TAMU experiments are:

- Rectangular test section, heated on one side. Unheated sections which can be used for adiabatic flow measurements
- Fairly long heated section (25.4cm)
- Very high PIV spatial resolution (0.1 pixel). Typical resolutions are 50-100 µ.
- In-house tracking routine to determine velocity from PIV images.
- PIV measurements will start with two velocity components, to be extended to 3-velocity components

2.1 Detailed experimental description

Geometry

Measurements are performed in a square channel test section of dimensions 10mm x 10mm x 305mm. This test section has one heated wall made of glass with an ITO deposited substrate with a resistance of 10 Ohms / in^2. Due to problems of undesired nucleation sites generated on the edge of the test section, part of the ITO substrate was removed from the left and right edges of the glass surface; also some length of the ITO heater was lost to allow space for the electrodes (see Fig. 1).

To ensure fully developed flow, an unheated section of dimensions 10mm x 10mm x 609 mm was used prior the test section. A metallic mesh was used to trip turbulence at the beginning of the unheated section. The relevant test section dimensions are listed in Table 1.

Table 1. Relevant experimental dimensions.

Parameter	Value	Comments
Length	305mm	
Width	10 mm	
Height	10 mm	
Heated Length	254 mm	
Heated Width	6.4 mm	
Heated Area	1625.6 mm^2	The heated area was reduced to avoid undesirable nucleation sites on the edge of the test section
Flow Area	100 mm^2	Cross sectional area
Non Heated Length	609 mm	Large heated length before the test section to ensure fully developed flow

Operational Conditions

To ensure the integrity of the test section (avoid reaching CHF or overpressure), only low Reynolds numbers and low heat flux experiments are performed. The operational conditions as of today are listed in Table 2.

Table 2. Experimental conditions at onset of nucleate boiling.

Parameter	Value
Voltage	61.0 V
Current	0.16 A
Output Power	8.14 W
Heat Flux*	**5.7 kW/m^2**
Volumetric Flow Rate	**1 Liter/min**
Reynolds number	**~4100**
Inlet Temperature	**25 C**

***Estimated heat flux without losses.**

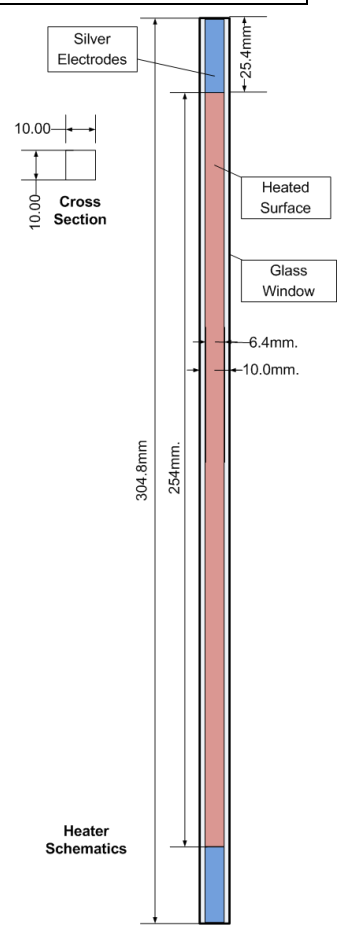

Fig. 1. Schematics of Test Section.

Table 3. Experimental parameters compared with PWR conditions.

Parameter	Experimental range	PWR range
Reynolds Number	0 - 3×10^4	2×10^5-5×10^5
Prandtl Number	5 – 7	0.9-1.2
Froude Number	0 – 2.6	0-217
Boiling Number	0 – 5.87×10^{-3}	0-0.25
Equilibrium Exit Quality	-0.27 - 0	-0.38 to -0.15
Liquid velocity (m/s)	0 – 1	2 - 5
Mass Flux (kg/m^{2}s)	0 - 1200	1500 - 3500
Temperature (°C)	10 - 150	286 - 324
Pressure (MPa)	0.1	15.5
Subcooling (°C)	0 – 30	21 - 58
Hydraulic Diameter (mm)	10	12
Wetted Perimeter (mm)	40	30
Heated Perimeter (mm)	10	30
Heat Flux (MW/m^2)	0 - 0.1	0 - 0.45
Channel Area (mm^2)	100	88

Although the heat flux is small, it is enough to obtain onset of subcooled boiling (for this low Reynolds number). For future experiments, a larger range of heat fluxes will be available with which we will ensure higher levels of boiling.

The anticipated departure bubble diameter size is about 0.15 – 2.0 mm. The bubble's departure diameter will depend on flow Reynolds number, wall heat flux, and subcooled level of the fluid. It can be estimated using the correlations summarized in Table 4. The minimum bubble diameter at a nucleation site to be registered is about 0.05 mm (50 μm).

Table 4. Summary of the models and correlation of bubble diameters in a vertical forced convective boiling.

Author	Model or correlation
Unal[6] (1976)	$D_{\max} = 2.42\times10^{-5}P^{0.709}\frac{a}{\sqrt{b\phi}}$, where $a = \frac{\Delta T_{sat}k_f\gamma}{2\rho_g h_{fg}(\pi\alpha_f)^{1/2}}$, $b = \frac{\Delta T_{sub}}{2(1-\rho_g/\rho_f)}$, $\gamma = (\frac{k_s\rho_s c_s}{k_f\rho_f c_{p,f}})^{1/2}$, $\phi = \max(\frac{U_{bulk}}{0.61}, 1)^{0.47}$
Prodanovic *et al.*[9] (2002)	$D_{lo}^{+} = 440.98\cdot Ja^{-0.708}\theta^{-1.112}(\frac{\rho_f}{\rho_g})^{1.747}Bo^{0.124}$, where $D_{lo}^{+} = \frac{D_{lo}\sigma}{\rho_f\alpha_f^2}$, $\theta = \frac{T_w - T_{bulk}}{\Delta T_{sat}}$, $Bo = \frac{q''}{Gh_{fg}}$
Situ *et al.*[10] (2005)	$D_{lo} = \frac{\sqrt{352/3}}{\pi}\frac{\nu_f}{u_r\sqrt{C_l}}b^2 Ja_e^2\,\mathrm{Pr}_f^{-1}$, where $u_r = u_f - u_b$, C_l: shear lift coefficient, b: bubble growth constant

Fig. 2. High speed visualization of nucleation sites to estimate average departure bubble diameters.

Bubble departure diameters are obtained experimentally and are defined as the average bubble diameter size at the instant that the bubble left the nucleation site. The departure bubble diameters are shown in Table 5. As we can observe, the bubble departure size depends on a specific nucleation site.

Table 5. Measured bubble departure diameters

Nucleation Site	Bubble Diameter
1	0.14 mm
2	0.30 mm
3	0.42 mm

2.2 Assumptions/Scaling/Approximations

The experimental facility was designed for the visualization of subcooled boiling flow of refrigerant HFE-301 at low system pressure. Refrigerant to water scaling analysis is given in the next section.

2.2.1 Fluid selection and scaling

The selection of the working fluid was based on a scaling analysis of thermodynamic properties. Scaling can be achieved by using critical fluid properties such as critical density, temperature or pressure. It has been shown (reference) that the critical pressure ratio p/p_c is the most useful parameter for many applications, including scaling between water and refrigerants. Scaling with the critical pressure ratio provided good similarity only for some fluid properties while for others a correction was needed. As an example, Fig. 3 shows the comparison of scaled thermodynamic properties of water and HFE-301 at saturation conditions. Fig. 3 (a) shows the two-phase flow density ratio (ρ_l/ρ_v) scaled with the critical pressure ratio. There is only a deviation of a few percent in the two-phase flow density ratio for water and HFE-301; however, when comparing the liquid viscosities μ_l in Fig. 3 (b), a larger discrepancy is found. A multiplication factor (k_4) is used to correct for this discrepancy. Fig. 3 (b) shows that liquid

viscosities for both fluids are comparable after applying the correction factor (black dotted line). This correction factor then must be considered in the estimation of dimensionless numbers. Also shown in Fig. 3 are three conditions on which HFE-301 may be used to simulate water. The Condition 1 simulates the behavior of a geometrically similar water system at a pressure of about 9 bars and saturation temperatures of 175 C. Conditions 2 and 3 are of importance for the nuclear industry, they represent typical operational conditions of Boiling and Pressurized Water Reactors (BWR, PWR) respectively. Table 6 shows saturation pressure and temperature values for both water and HFE-301 for each condition.

Table 6: Important operation conditions and corresponding values for HFE-301 refrigerant and water

Condition No.	P_{HFE}[bar]	$Tsat_{HFE}$[°C]	P_{H_2O}[bar]	$Tsat_{H_2O}$[°C]
1	1.00	36.00	8.95	175.13
2	7.80	107.00	70.00	285.83
3	16.08	141.00	140.00	336.67

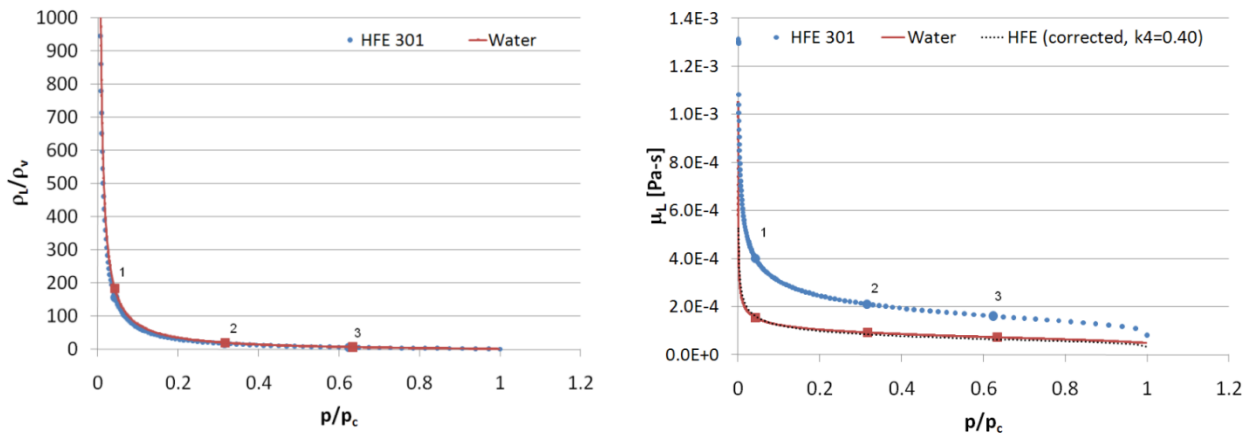

(a) (b)

Fig. 3. Important operation conditions and corresponding values for HFE-301 refrigerant and water.

3. Simulation definition

3.1 Operating conditions

To simplify the experimental validation, the challenge simulation will use the refrigerant properties as in the TAMU experiment. The simulation will be performed for statistically steady-state flow conditions; however the void fraction will vary stream-wise due to the heat flux from the wall in the saturated liquid.

3.2 Domain

The goal of the simulation is to capture the process of subcooled boiling to be observed in the TAMU experiments. While the experimental heated section is 220 mm long, the proposed domain length is 100mm. It will allow estimating shorter/longer domain sizes / computational costs easily, and determining final simulation domain based on the experimental results pattern (e.g. we are not

interested in flow regime transition within the scope of this challenge problem should it occur at certain distance of the heated section).

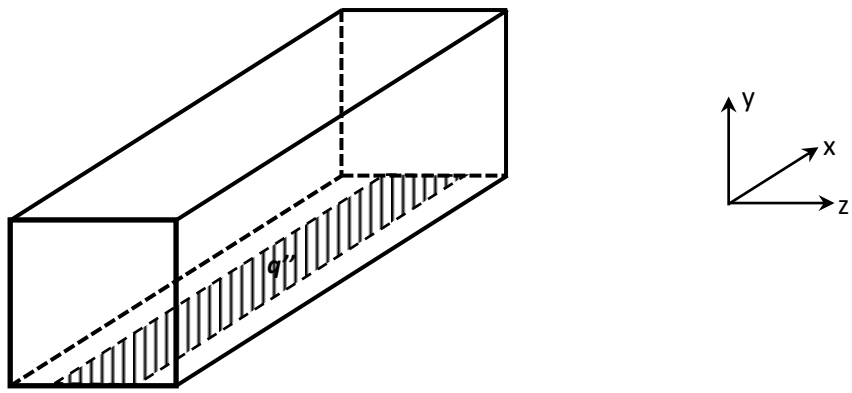

Fig. 4. Two-phase computational domain geometry and axis orientation

Computational domain schematic with a heated section is shown in Fig. 4 and the coordinates range are in Table 7.

Table 7. Computational domain boundaries

Axis	Left boundary	Right boundary
X	L_{x0} = 0.0 mm	L_{x1} = 100.0 mm
Y	L_{y0} = -5.0 mm	L_{y1} = 5.0 mm
Z	L_{z0} = -5.0 mm	L_{z1} = 5.0 mm

3.3 Boundary conditions

Developing boiling flow simulations cannot be performed with periodic boundary conditions in the stream-wise direction. Single-phase liquid turbulent inflow will be used and two-phase bubbly mixture will exit the domain at the outflow. To properly resolve turbulent structures full cross-section (10 mm * 10 mm) will be modeled with no-slip wall boundary conditions.

Constant heat flux is applied to the heated section of the wall and is measured experimentally based on the voltage and current provided by the power-supply. The heat flux can be estimated as follows:

$$\dot{q}''_H = \frac{VA}{A_H}$$

where V and A is the voltage drop and the current across the heater, respectively, and A_H is the heated area. The correctness or uncertainty of evaluating heat flux in this manner can be determined from single-phase heated flow experiments by measuring the temperature and liquid flow distribution using thermocouples and the PTV technique, respectively. Such tests will give us the information of the amount of heat that is transferred to the fluid compared to the one provided by the power-supply.

The heat loss to the atmosphere (from the back of heater) is expected to be negligible because the heat transfer to the environment is prevented with insulation in our experiment (e.g. BaF2 window is installed close to the heater to prevent the heat loss to the environment). In this context, the adiabatic boundary condition might be an appropriate option for the simulation of flow-boiling experiment. Detailed information on the heat flux and heat losses measurements and their uncertainties are provided in [2].

3.3.1. Conjugate Heat Transfer

While the insulation behind the heater and low temperature difference with the environment (due to using a refrigerant) minimizes the heat loss, it will be valuable to test the effect of the insulation below the ITO heater (Fig. 5).

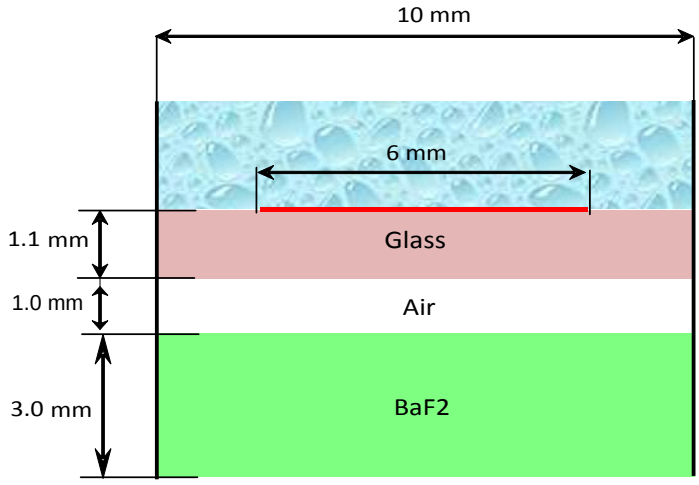

Fig. 5. Cross-section view of the ITO heater (red line) and insulating glass (pink rectangle), air gap (white) and Barium Fluoride window (green). Bubble pattern shown only for the purpose of designating the two-phase flow region.

The nucleation of the individual bubbles creates local temperature gradients within the channel wall (below the heating surface). While the modeling of the conjugate heat transfer may provide some challenges for ITM, it is highly recommended to evaluate the influence of the insulating walls. If it can be shown that difference in bubble's behavior for two simulations with and without the conjugate heat transfer is small, and negligible compared to other sources of uncertainties in ITM, the additional effort and costs associated with implementation and modeling of CHT should be taken into consideration.

3.3.2. Single-phase turbulent inflow boundary condition

In order to provide physically correct turbulent inflow boundary conditions a supplemental single-phase simulation in a periodic domain can be developed.

The purpose of the supplemental case is to record fluctuating velocity components at the lateral coordinates corresponding to the nodes at the inflow plane of the two-phase case of interest. The recorded data is then used in the two-phase simulation as the inflow boundary conditions.

3.4 Initial conditions

For such complex transient flow phenomena a boiling flow a substantial simulation time is required to achieve meaningful results. Thus, the initial conditions will ensure the presence of turbulence and ability to resolve the bubbles which will be generated. More important will be the quality inflow boundary conditions discussed in section 3.3.

Based on the nucleation site density data, pre-determined nucleation sites will be embedded in the flow geometry which can be activated and de-activated based on the wall super-heat.

3.5 Grid Size

3.5.1. Turbulence resolution requirements-based mesh

To ensure that the proper computational grid resolution to fully resolve all turbulence fluctuations, the following mesh structure will be used:

- First node off the wall is at $y^+ = 0.5$
- Boundary layer growth rate: $\frac{dy_{i+1}^+}{dy_i^+} = 1.1$, where $dy_i^+ = y_i^+ - y_{i-1}^+$
- Maximum value in outside the boundary layer mesh: $dy^+ = 6.0$
- Stream-wise resolution: $dx^+ = 8.0$

  Note that the viscous length scale (y_i^+ unit) is defined as

$$\delta_\nu = \frac{\nu}{u_\tau} \tag{1}$$

Here friction velocity is defined using wall shear stress:

$$u_\tau = \sqrt{\frac{\tau_w}{\rho}} \tag{2}$$

Darcy friction factor is estimated from Colebrook equation:

$$\frac{1}{\sqrt{f}} = -2.0\log\left(\frac{\varepsilon/D}{3.7} + \frac{2.51}{\mathrm{Re}\sqrt{f}}\right) \tag{3}$$

where roughness, ε, is assumed 0 in this case. Wall shear stress is then determined as:

$$\tau_w = \rho U^2 \frac{f}{8} \tag{4}$$

Assuming that the average resolution in the non-stream-wise directions is $dy^+ = 3.0$ the mesh sizes are estimated for a range of Reynolds number expected to be achieved in the experiments (Table 8).

Table 8. Estimated grid resolutions based on the different Reynolds numbers.

Re:	4,100	10,000	20,000	30,000
Re_τ:	144	310	568	812
Viscous unit:	0.035	0.0161	0.0088	0.0061
dx (8vu):	0.28	0.1288	0.0704	0.0488
dy (3vu):	0.105	0.0483	0.0264	0.0183
dz (3vu):	0.105	0.0483	0.0264	0.0183
Nx	357	776	1420	2049
Ny	95	207	379	546
Nz	95	207	379	546
Ntotal	3,239,391	33,280,503	203,807,183	611,896,542

3.5.2. Bubble resolution requirements-based mesh

We assume that **18 points** across the bubble diameter is required to fully resolve a single bubble using the ITM, such as level set method (Bolotnov, et al., 2011). The summary of computational mesh size estimates which satisfy bubble resolution requirements for different fully resolved minimum bubble sizes (anything smaller than specified size is not fully resolved) is provided in Table 9.

Table 9. Bubble-sized based resolution estimates:

Bubble size:	Mesh resolution:	X-res:	Y-res:	Z-res:	Mesh size:
0.50	0.027777778	3600	360	360	466,560,000
1.00	0.055555556	1800	180	180	58,320,000
1.50	0.083333333	1200	120	120	17,280,000
2.00	0.111111111	900	90	90	7,290,000

3.5.3. Mesh Adaptivity

For unstructured meshes it is possible to apply mesh adaptivity in order to relax bubble resolution restrictions in all regions where bubbles are not observed.

Advanced meshes for nucleating bubbles

Provided we know the anticipated departure diameter and prescribe the nucleating sites, the bubble growth can be affordable to model starting with very small bubbles. While the departed bubbles must be resolved in the flow domain, the nucleating bubbles only require the resolution *at the nucleating sites*. Let's assume that a bubble is seeded with diameter of D_s and grows to the size of D_b. The 3D domain region surrounding the nucleation site must resolve the smallest bubble with N_b points, however the resolution requirement for the largest bubble is also N_b. The adapted mesh size resolution for this region in the domain can be estimated as:

$$\Delta x_i(r_n) = \max\left(\frac{r_n}{N_b}, \frac{D_s}{N_b}\right) \tag{5}$$

where r_n is the distance to the nucleation site.

Table 10 summarizes the additional meshing requirements for various bubble sizes using the adaptive meshing approach. As one can see even with hundreds of pre-defined nucleating sites the additional meshing requirements are affordable (100 nucleation sites will add 6 million elements to the 466M mesh and ensure the bubbles growing from 0.05mm to the 0.5mm departure diameter). Note that we do not expect experimental results to provide any information about the bubbles smaller than 50 μm (0.05 mm) as they nucleate. In the near future, better resolution might be provided, if needed. In this case finer meshes may be employed.

Table 10. Adaptive meshing requirements for individual nucleation sites.

Bubble seed size:	Bubble departure size:	Points per diameter:	Additional mesh cost per nucleation site:
0.05	**0.5**	18	128,156
0.05	**1.0**	18	234,360
0.1	**0.5**	18	59,584
0.1	**1.0**	18	128,156
0.2	**0.5**	18	24,520
0.2	**1.0**	18	59,584
0.1	**0.5**	16	46,620
0.1	**1.0**	16	95,500
0.2	**0.5**	16	17,604
0.2	**1.0**	16	46,620

3.5.4. Proposed cases which fully resolve both turbulence and bubbles

In order to separately validate ITM code capabilities it is proposed to perform no-phase-change simulations before the boiling/condensation phenomena is modeled. Thus, the following 2 types of cases will be considered:

- no-phase-change bubbly flow simulation (20M mesh)
- nucleation boiling simulations
    - preliminary validation case (5M mesh)
    - large scale simulation (200M mesh)
    - detailed bubble resolution simulation (1,100M mesh)

To reconcile the differences between the turbulence and bubbly flow resolution requirements we have to satisfy both for certain Reynolds numbers and bubble sizes. Also, we defined three boiling cases with different computational costs. The less expensive case will be used for preliminary validation of DNS models as well as testing and calibration of upscaling tools. The more computationally expensive cases will be used for full comparison with experimental data and generating detailed numerical database for CFD model development and DNS upscaling.

Let's describe each of these cases in more detail:

No-phase-change case:

The first simulation case should be based on the unheated section of the experimental facilities where the bubbles are present: downstream of the heated section. The length of the computational domain depends in the condensation rate of the bubbles so the no-phase-change assumption can be applied.

The bubbles size distribution can be estimated from experiments. Cross sectional visualization on the unheated section were performed at 48 cm or 48 hydraulic diameters (D_h) after the heated length using a high speed camera and a boroscope lens. Fig. 6 shows experimental images from which bubbles diameters can be obtained. Table 11 shows the measured bubbles diameters estimated from Figure 5.

Table 11. Measured bubble diameters at 40 D_h downstream the heated section

Nucleation Site	Bubble Diameter
1	1.57 mm
2	1.05 mm
3	0.95 mm

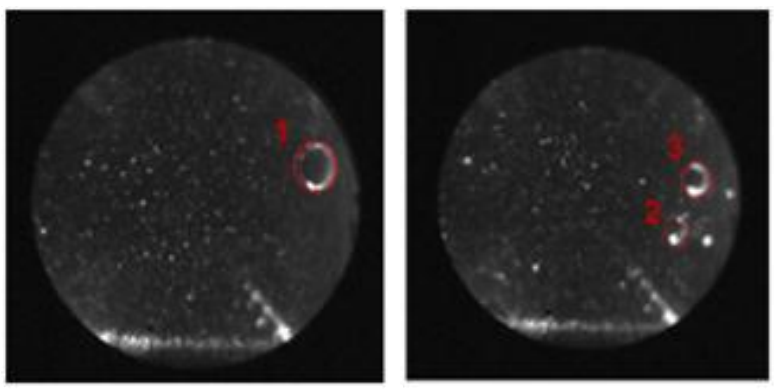

Fig. 6. High speed Boroscope visualization of boiling bubbles on the non-heated section

Note: the experimental results are not yet finalized; automatization of algorithms to process the boroscope experimental images will provide full bubble size distributions.

Preliminary validation case:

We will use the smaller domain length, L_{x1} = 20.0 mm for this case and require 1.5 mm bubbles to be fully resolved. Based on this information the following grid parameters are estimated:

- ReD = 4,100
- Re_τ = 144
- dx = 0.083 mm (required to resolve 1.5 mm bubbles)
- average dy = dz = 0.073 mm based on 1.1 B.L. growth rate and maximum value of 0.083 mm for bubble resolution (dy^+_1 = 0.5)

The resulting mesh size is 4.5 M hexahedral elements (241x137x137).

Optional: Adapted mesh for 2 nucleation sites with 0.5 mm seed bubble diameter.

Large scale simulation:

We will use the full domain length, L_{x1} = 220.0 mm for this case and require 1.0 mm bubbles to be fully resolved. Based on this information the following grid parameters are estimated:

- ReD = 20,000
- Re_τ = 568
- dx = 0.055 mm (required to resolve 1.0 mm bubbles)
- average dy = dz = 0.0463 mm based on 1.1 B.L. growth rate and maximum value of 0.055 mm for bubble resolution (dy^+_1 = 0.5)

The resulting mesh size is 187 M hexahedral elements (4000x216x216).

Optional: Adapted mesh for 10 nucleation sites with 0.5 mm seed bubble diameter. Additional cost of 2.34 million elements. The location of nucleation sites will be determined based on the experimental observations.

Fig. 7 shows two different nucleation sites at different locations along the heater wall.

(a) 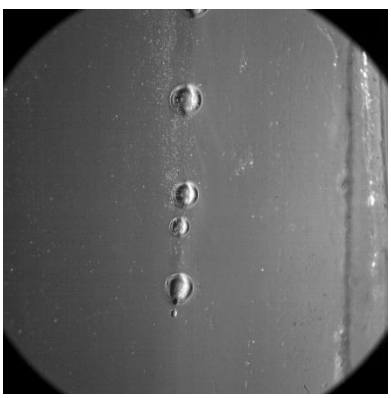 (b) 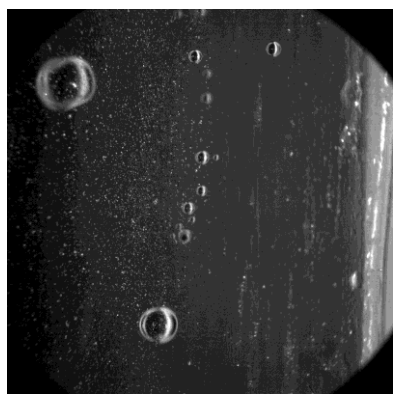

Fig. 7. Zoom images of nucleation sites located at (a) six hydraulic diameters, (b) 9 hydraulic diameters from the start of heating.

Detailed bubble resolution simulation:

We will use the full domain length, L_{x1} = 220.0 mm for this case and require 0.5 mm bubbles to be fully resolved. Based on this information the following grid parameters are estimated:

- ReD = 20,000
- Re_τ = 568
- dx = 0.0278 mm (required to resolve 0.5 mm bubbles)
- average dy = dz = 0.0261 mm based on 1.1 B.L. growth rate and maximum value of 0.0278 mm for bubble resolution (dy^+_1 = 0.5)

The resulting mesh size is 1,162 M hexahedral elements (7914x383x383).

Optional: Adapted mesh for 50 nucleation sites with 0.05 mm seed bubble diameter. Additional cost of 6.0 million elements. The location of nucleation sites can be determined based on the experimental observations or seeded randomly with appropriate probability based on experimental patterns.

For successful bubble tracking the number of nucleation sites will be kept within 10. More sites will result in a more complex pattern and high void fraction of the flow. Those conditions should be used to CMFD evaluation. Averaged quantities (such as void fraction and mean velocity) can be obtained from both high-void fraction experiments and large scale ITM simulations and cross compared.

Table 12. Summary of the challenge simulation cases.

Case Name:	X-res:	Y-res:	Z-res:	Mesh size:	Number of cores[1]:
Preliminary	241	137	137	4,521,746	560
Large scale	4000	216	216	186,594,144 (+2.34M adaptive)	23,312
Highly detailed	7914	383	383	1,161,707,706 (+6.0M adaptive)	145,200

The major reason for further mesh growth will be increased requirements for bubble resolution. This can be partially mitigated by using the adaptive mesh techniques as summarized in the table.

4. Requested calculations and metrics

The following quantities and correlations will be collected and computed from the challenge problem simulations (this list should be updated based on the upscaling definitions and discussions). For large scale simulation up to 5 measuring stations will be chosen axially. At each station the following profiles will be measured:

- Mean velocity for liquid and gas (including normal to the heated wall velocities)
- Liquid turbulent kinetic energy
- Reynolds stress components (liquid and gas data)
- Bubble volume fraction
- Budget of turbulent kinetic energy
- Heat transfer coefficient
- Velocity gradient information

[1] Based on 8,000 elements per processor assumption and rounded to 16 cores per nodes (XK6 “Titan” architecture)

5. Upscale of results to multiphase CFD level

The purpose of the detailed proposed DNS study is to provide information for informing the coarse scale models. This section will discuss possible approaches on how to effectively utilize the multiphase DNS data.

Proposed path:

- Identify the multiphase turbulence CFD model to be used for the upscaling exercise (high-Re k-ε w/ two-phase modifications can be the first candidate)
- Perform the challenge simulations outlined in this report.
- Advanced two-phase flow statistics can be collected, the set of data to be recorded would allow DNS-based CFD model validation by verifying the model's source terms and evaluating it using the DNS data (see the example).
- Model modifications / new modeling forces will be proposed based on the DNS-sourced results
- Both the original multiphase model formulation and modified version will be used to run the same case using two-fluid CMFD approach (e.g. NPHASE or other code if available) and compared with the averaged DNS results.
- Successful demonstration will lead to specifying a wider range of future DNS simulations to test the model behavior at different void fractions, non-adiabatic conditions etc.

Example: Evaluate the turbulent viscosity prediction for two-phase bubble flow.

DNS information:

- turbulent kinetic energy can be extracted as: $k^k(t) = \frac{1}{\alpha_k N_e} \sum_{m=1}^{N_e} \left(\frac{1}{N_w} \sum_{j=1}^{N_w} X_k \sum_{i=1}^{3} \frac{1}{2} \left(u_m'^i (t+t_j) \right)^2 \right)$
- dissipation rate: $\varepsilon^k(t) = \nu \frac{1}{\alpha_k N_e} \sum_{m=1}^{N_e} \left(\frac{1}{N_w} \sum_{j=1}^{N_w} \sum_{i=1}^{3} \sum_{k=1}^{3} X_k \left(\frac{\partial u_m'^i (t+t_j)}{\partial x_k} \right)^2 \right)$
- turbulent shear stress: $\tau_{xy}^k(t) = \frac{1}{\alpha_k N_e} \sum_{m=1}^{N_e} \left(\frac{1}{N_w} \sum_{j=1}^{N_w} X_k u_m'^x (t+t_j) u_m'^y (t+t_j) \right)$
- turbulent viscosity: $\nu_T^{DNS} = \tau_{xy} \Big/ \frac{dU}{dy}$

CMFD model information:

- based on DNS data: $\nu_T^{k-\varepsilon} = C_\mu \frac{k^2}{\varepsilon}$, where k and ε come from DNS data
- based on CMFD code results: $\nu_T^{CMFD} = C_\mu \frac{k^2}{\varepsilon}$, where k and ε come from the solution of the equations

By obtaining the described statistics model constants can be adjusted to obtain better results (in this case C_μ can be fitted). Since the k and ε distributions depend on the formulation of other terms in the R.H.S. of these equations, higher order statistics will be collected (production, diffusion terms) and term-by-term evaluation will be performed.

Bibliography

[1] Mayinger, F., 1981. *Two-Phase Flow and Heat Transfer in the Power and Process Industries*. Vol. 1. Hemisphere Publishing Corporation, Washington, D.C., Ch. Scaling and modeling laws in two-phase flow and boiling heat transfer, pp. Chap. 14, 424-454.

[2] C. E. Estrada Perez, *Experimental Two-Phase Flow Characterization of Subcooled Boiling in a Rectangular Channel*. College Station, TX: Texas A&M University, 2010.